KSME

Springer

Journal of Mechanical Science and Technology 34 (2) 2020

Original Article
DOI 10.1007/s12206-020-0135-2

Keywords:
· Autonomous surface vehicles
· Position tracking control
· Dynamic surface control
· Neural network
· State predictor

Correspondence to:
Cong Wang
alanwang@hit.edu.cn

Citation:
Zhang, C., Wang, C., Wei, Y., Wang, J. (2020). Neural network adaptive position tracking control of underactuated autonomous surface vehicle. Journal of Mechanical Science and Technology 34 (2) (2020) 855~865.
http://doi.org/10.1007/s12206-020-0135-2

Received June 27th, 2019
Revised September 18th, 2019
Accepted December 5th, 2019

† Recommended by Editor Ja Choon Koo

Neural network adaptive position tracking control of underactuated autonomous surface vehicle

Chengju Zhang, Cong Wang, Yingjie Wei and Jinqiang Wang

School of Astronautics, Harbin Institute of Technology, Harbin, 150001, China

Abstract The present study investigates the position tracking control of the underactuated autonomous surface vehicle, which is subjected to parameters uncertainties and external disturbances. In this regard, the backstepping method, neural network, dynamic surface control and the sliding mode method are employed to design an adaptive robust controller. Moreover, a Lyapunov synthesis is utilized to verify the stability of the closed-loop control system. Following innovations are highlighted in this study: (i) The derivatives of the virtual control signals are obtained through the dynamic surface control, which overcomes the computational complexities of the conventional backstepping method. (ii) The designed controller can be easily applied in practical applications with no requirement to employ the neural network and state predictors to obtain model parameters. (iii) The prediction errors are combined with position tracking errors to construct the neural network updating laws, which improves the adaptation and the tracking performance. The simulation results demonstrate the effectiveness of the proposed position tracking controller.

1. Introduction

In the last few decades, the motion control of autonoumous surface vehicles (ASVs) has attracted many scholars. Since ASVs have good flexibility, multipurpose applications and strong endurance, they can be employed to monitor the environment, explore marine sources, replenish the energy for other vehicles and so on [1-4]. However, most of the ASVs are underactuated, which indicates that the number of control inputs is less than the degrees of freedom. This can be interpreted as the existence of strong couplings between the degrees of freedom. Moreover, strong nonlinear external disturbances are a main challenge for ASVs, which are induced by ocean currents, waves and winds [5]. Therefore, the position tracking of the underactuated ASVs is a challenging problem in the marine structures.

In order to solve the motion control of the underactuated autonomous surface vehicles, different control schemes have been designed so far for the tracking problem [6-11]. Bi et al. [12] proposed a backstepping controller to solve the position tracking problem of the underactuated ASVs on the horizontal plane. Moreover, Pan et al. [13] developed an adaptive robust controller based on the backstepping method, single-layer neural network and the Lyapunov stability theory for the underactuated ASVs. However, the nonlinear external disturbances are not considered in this study. In Ref. [14], an adaptive neural network control scheme was designed to solve the position tracking problem of the underactuated ASVs. However, this scheme could not reduce the computational complexities of the conventional backstepping method. In Ref. [15], a neural-adaptive controller was proposed to track a desired trajectory for the underactuated ASVs. However, only the unknown ocean currents were considered in the designed controller, while other disturbances were neglected. Furthermore, Do et al. [16] proposed a global robust adaptive controller to track a desired path for underactuated ASVs considering the time-varying disturbances. They conducted simulation and experiments to prove the effectiveness of the proposed controller. However, they didn't consider uncertainties of parameters. Furthermore, a global tracking controller was presented to track a desired trajectory of underactuated nondiagonal ASVs in Ref. [17]. However, the controller was only applied to small nondiagonal ASVs, so it ignored uncertainties of the parameters. Xie et al. [18] proposed a cascaded control scheme to follow the desired trajectory of the underactuated ASVs based on the non-diagonal inertia and damping. However, the nonlinear external disturbances were not considered in the control system. Swaroop et al. [19] presented the dynamic surface control (DSC) to avoid the explosion of complexities of the conventional backstepping method so that the derivative of the virtual variables are obtained by a first-order filter. Moreover, Wang et al. [20] proposed an adaptive neural network tracking controller to realize the trajectory tracking of the underactuated AUVs. The radial basis function neural network (RBFNN) was adopted to estimate and compensate uncertainties of model parameters. However, errors between uncertain functions and the estimation model were not taken into the consideration. In Ref. [21], an adaptive sliding mode technique was designed to solve the nonlinear external disturbances. Moreover, an adaptive nonlinear robust control scheme was proposed to realize the path following for the underactuated autonomous underwater vehicles by employing backstepping method and sliding mode control in Ref. [22]. However, the damping matrix was only compensated by the adaptive law, while other uncertainties of parameters were ignored. Zheng et al. [23] designed an adaptive neural network controller to compensate uncertainties of the parameters and input saturation of the underactuated ASVs. However, the designed control scheme has unjustifiable computational complexity. Wang et al. [24] designed a nonlinear robust control scheme to follow the desired path of underactuated autonomous surface vehicles. Then, a feedback gain controller was designed to track a desired path of the underactuated ASV in the horizontal plane in Ref. [25]. However, the controller can be carried out with accurate model parameters. In Ref. [26], the command filtered backstepping method was presented to follow the desired path of the underactuated autonomous underwater vehicles. However, parameters uncertainties and the nonlinear external disturbances were not taken into consideration, which limits its real applications. Furthermore, a neural network robust controller was developed for underactuated ASVs in Ref. [27]. The control system can be effective to the dynamic uncertainties and external disturbances. In Ref. [28], an adaptive controller was designed to realize the trajectory tracking of the ASVs. However, parameters uncertainties were not considered. In Ref. [29], an adaptive output feedback control scheme was proposed to track the trajectory of the underactuated ASVs. The control system considered the underactuated ASVs model, where the mass and damping matrices were not diagonal. However, the nonlinear external disturbances were not taken into the consideration. Liu et al. Ref. [30] presented a neural network control scheme to track a desired trajectory of the underactuated ASVs. The neural network was constructed to provide an estimation of the unknown disturbances. However, parameters parameters were ignored.

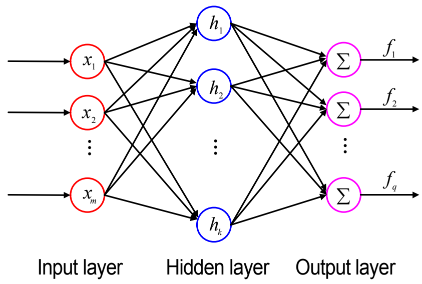

Fig. 1. Structure of the three-layer RBF neural network.

In the present study, it is intended to propose an adaptive position tracking control scheme for the underactuated ASVs in the presence of uncertainties of the parameters and nonlinear external disturbances.

The rest of this article is arranged as follows. In Sec. 2, the position tracking problem, kinematic model, dynamic model, and error equations of underactuated ASVs are introduced. Moreover, the neural network adaptive robust controller of underactuated ASVs is designed in Sec. 3. Then, the Lyapunov function is applied in Sec. 4 to prove the stability of the closed loop control system. In Sec. 5, simulation results, comparative analysis and the position tracking performance of the designed controller are presented. Finally, the conclusion of the article is presented in Sec. 6.

2. ASV modelling and problem formulation

2.1 The neural networks

The neural network has numerous intrinsic abilities in the function approximation. Therefore, it plays an important role in the robotic control. In this section, a radial basis function neural network (RBFNNs) with linear parameterization and simple mechanism [31] is introduced. Fig. 1 shows the typical three-layer RBFNN, which is applied in the present study to solve the model uncertainties

$$\begin{aligned} f(\mathbf{x}) &= \mathbf{W}\mathbf{h}(\mathbf{x}) + \varepsilon \\ h(\mathbf{x}) &= \exp\left(\frac{\left\|\mathbf{x}-\mathbf{c}_j\right\|^2}{2\mathbf{b}_j^2}\right) \end{aligned} \tag{1}$$

where $\mathbf{x}, \mathbf{W}$ and $\mathbf{h}(\mathbf{x})$ denote the input vector of the RBFNN, the weight adjustment and the Gaussian basis function, respectively. Moreover, $\mathbf{c}_j$ and $\mathbf{b}_j$ represent a *j*-dimensional vector denoting the center of the j^{th} basis function and the standard deviation, respectively.

$$f^*(\mathbf{x}) = \mathbf{W}^*\mathbf{h}(\mathbf{x}) + \varepsilon \tag{2}$$

where $\mathbf{W}^*$ indicates the optimal weight adjustment.

$$\hat{f}(\mathbf{x}) = \hat{\mathbf{W}}\mathbf{h}(\mathbf{x}) + \varepsilon \tag{3}$$

where $\hat{f}$ and $\hat{\mathbf{W}}$ denote the NN output and the estimation of the weight adjustment, respectively.

Assumption 1. The ideal weight matrix $\mathbf{W}^*$ and the approximation error ε are bounded so that there are W_M and ε_M, $\|\mathbf{W}^*\| \le W_M$ and $\varepsilon \le \varepsilon_M$ [21].

2.2 The underactuated ASV model

The kinematic and dynamic models are presented in this section. In order to simplify the derivation of the equation, the mass and the damping matrices are regarded to be diagonal. Moreover, external disturbances are taken into consideration for the underactuated ASV model. The kinematic and dynamic models are described as follows [32]:

$$\begin{cases} \dot{\boldsymbol{\eta}} = \boldsymbol{J}(\psi)\boldsymbol{v} \\ \boldsymbol{M}\dot{\boldsymbol{v}} + \boldsymbol{C}(\boldsymbol{v})\boldsymbol{v} + \boldsymbol{D}\boldsymbol{v} = \boldsymbol{\tau} + \boldsymbol{\tau}_e \end{cases} \tag{4}$$

where

$$\boldsymbol{\eta} = [x\ y\ \psi]^T \quad \boldsymbol{v} = [u\ v\ r]^T$$
$$\tau = [\tau_u\ 0\ \tau_r]^T \quad \tau_e = [\tau_{eu}\ \tau_{ev}\ \tau_{er}]^T$$
$$\boldsymbol{J}(\psi) = \begin{bmatrix} \cos\psi & -\sin\psi & 0 \\ \sin\psi & \cos\psi & 0 \\ 0 & 0 & 1 \end{bmatrix} \tag{5}$$
$$\boldsymbol{M} = \begin{bmatrix} m - X_{\dot{u}} & 0 & 0 \\ 0 & m - Y_{\dot{v}} & 0 \\ 0 & 0 & m - N_{\dot{r}} \end{bmatrix} = \begin{bmatrix} m_{11} & 0 & 0 \\ 0 & m_{22} & 0 \\ 0 & 0 & m_{33} \end{bmatrix} \tag{6}$$
$$\boldsymbol{C}(\boldsymbol{v}) = \begin{bmatrix} 0 & 0 & -m_{22}v \\ 0 & 0 & m_{11}u \\ m_{22}v & -m_{11}u & 0 \end{bmatrix} \tag{7}$$
$$\boldsymbol{D} = \begin{bmatrix} X_u + X_{u|u|}|u| & 0 & 0 \\ 0 & Y_v + Y_{v|v|}|v| & 0 \\ 0 & 0 & N_r + N_{r|r|}|r| \end{bmatrix} \tag{8}$$

where x, y and ψ denote positions and orientations of underactuated ASVs in the earth fixed frame, respectively. Moreover, u, v and r denote the surge, sway and yaw velocities in the body fixed frame, respectively. X_u, Y_v, N_r, $X_{u|u|}$, $Y_{v|v|}$ and $N_{r|r|}$ denote the hydrodynamic parameters. $m_{ii}(i = 1,2,3)$ denote the combined inertia and added mass terms in the body fixed frame. τ_u and τ_r denote control force and control force moment, respectively. τ_{eu}, τ_{ev} and τ_{er} denote the ocean disturbances induced by ocean currents, waves and wind.

Assumption 2. The ocean disturbances are bounded when $|\tau_{ek}| \le \tau_e^*$, where $k = u,v,r$ and τ_e^* represents an unknown positive constant [35].

Assumption 3. The yaw angle of the underactuated ASV is bounded so that $|\psi| \le \psi_{\max} < \pi/2$ to ensure the system stability in the controller [12].

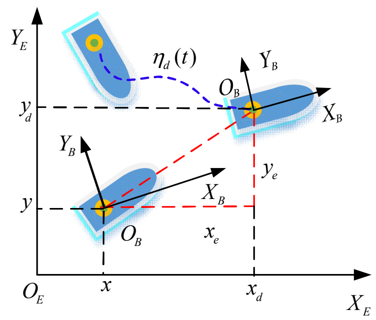

Fig. 2. The ASV frames in the position tracking problem.

Assumption 4. $\boldsymbol{\eta}_d = [x_d\ y_d\ \psi_d]^T$ is a smooth desired trajectory and its derivatives are time-varying bounded [12].

Assumption 5. The velocity of the underactuated ASV in the sway is bounded so that $\sup_{t\ge0}|v| \le v_M$ and the error of v is not stable in the epilogue [35].

2.3 Error dynamics of the position tracking problem

In order to facilitate the problem formulation, the frame is designed to position the tracking of underactuated ASV. Fig. 2 shows the designed frame. It should be indicated that $\{O_E, X_E, Y_E\}$ and $\{O_B, X_B, Y_B\}$ denote the earth fixed frame and the body fixed frame, respectively. Moreover, $\{x_d, y_d\}$ and $\{x, y\}$ denote the desired position and the coordinate of Q in the geodetic fixed frame, respectively. Furthermore, $\{x_e, y_e\}$ and $\{e_x, e_y\}$ represent the errors of the position tracking in the earth fixed frame and in the body fixed frame, respectively.

The position tracking errors in the earth fixed frame are defined as follows

$$x_e = x_d - x \quad y_e = y_d - y \tag{9}$$

Then, Eq. (6) can be converted to the following equations:

$$\begin{cases} e_x = x_e\cos\psi + y_e\sin\psi \\ e_y = -x_e\sin\psi + y_e\cos\psi \end{cases} \tag{10}$$

where e_x and e_y denote the position tracking errors in the body fixed frame.

Eq. (10) indicates that errors of the earth fixed frame and the body fixed frame are equivalent, which is described as the following:

$$\begin{cases} x_e(t) = 0 \\ y_e(t) = 0 \end{cases} \Leftrightarrow \begin{cases} e_x(t) = 0 \\ e_y(t) = 0 \end{cases} \tag{11}$$

The control object is designing control inputs τ_u and τ_r, where the aim is approaching tracking errors e_x and e_y to zero. Differentiating Eq. (10) along with Eq. (4) yields:

$$\begin{cases} \dot{e}_x = -u + v_m \cos\psi_e + re_y \\ \dot{e}_y = -v + v_m \sin\psi_e - re_x \end{cases} \tag{12}$$

where $v_m = \sqrt{\dot{x}_d^2 + \dot{y}_d^2}$.

3. Controller design

In this section, a position tracking controller is designed based on the backstepping method, adaptive control techniques and neural network. It is indicated that the position tracking, surge velocity, auxiliary variable and yaw velocity errors are stabilized in steps 1, 2, 3, and 4, respectively. Moreover, adaptive control laws of the neural network are designed in step 5.

Step 1: In order to stabilize the position tracking errors, a Lyapunov function is defined as the following:

$$V_1 = \frac{1}{2}(e_x^2 + e_y^2) \tag{13}$$

Differentiating Eq. (13) along with Eq. (12) yields the equation below:

$$\begin{aligned} \dot{V}_1 &= e_x\dot{e}_x + e_y\dot{e}_y \\ &= e_x(-u + v_m\cos\psi_e + re_y) + e_y(-v + v_m\sin\psi_e + re_x) \\ &= e_x(-u + v_m\cos\psi_e) + e_y(-v + v_m\sin\psi_e) \end{aligned} \tag{14}$$

In order to facilitate the formula derivation, a new auxiliary variable is defined as follows:

$$\upsilon = v_m \sin\psi_e \tag{15}$$

To ensure $\dot{V}_1 \le 0$, u and υ are considered as virtual variables and their desired values are designed as:

$$\begin{cases} u_c = \lambda_1 e_x + v_m\cos\psi_e \\ \upsilon_c = -\lambda_2 e_y + v_m \sin\psi_e \end{cases} \tag{16}$$

where λ_1 and λ_2 are positive constants.

Substituting Eq. (16) into Eq. (14) yields:

$$\dot{V}_1 = -\lambda_1 e_x^2 - \lambda_2 e_y^2 \tag{17}$$

In order to avoid the computational explosion, $u_c(t)$, $\upsilon_c(t)$ and $r_c(t)$ should pass the following first-order filter [33].

$$\begin{cases} k_u\dot{u}_{cf}(t) + u_{cf}(t) = u_c(t) \\ k_\upsilon\dot{\upsilon}_{cf}(t) + \upsilon_{cf}(t) = \upsilon_c(t) \\ k_r\dot{r}_{cf}(t) + r_{cf}(t) = r_c(t) \end{cases} \tag{18}$$

where k_u, k_υ and k_r are positive constants, which are selected later, and $u_{cf}(0) = u_c(0)$, $\upsilon_{cf}(0) = \upsilon_c(0)$, $r_{cf}(0) = r_c(0)$ $u_{cf}(t)$, $\upsilon_{cf}(t)$ and $r_{cf}(t)$ denote the filtered signals.

Step 2: The error variables are defined as:

$$e_u = u - u_{cf} \quad e_\upsilon = \upsilon - \upsilon_{cf} \quad \zeta_u = u_c - u_{cf} \tag{19}$$

Then, Eq. (17) can be converted to the following equation:

$$\dot{V}_1 = -\lambda_1 e_x^2 - \lambda_2 e_y^2 - e_u e_x + e_\upsilon e_y + \zeta_u \dot{\zeta}_u \tag{20}$$

Then, a new Lyapunov function can be defined as:

$$V_2 = V_1 + \frac{1}{2}\left(e_u^2 + \zeta_u^2\right) \tag{21}$$

Differentiating Eq. (21) along with Eq. (20) yields:

$$\begin{aligned} \dot{V}_2 &= \dot{V}_1 + e_u\dot{e}_u + \zeta_u\dot{\zeta}_u \\ &= -\lambda_1 e_x^2 - \lambda_2 e_y^2 + e_u(\dot{e}_u - e_x) + e_\upsilon e_y + \zeta_u\dot{\zeta}_u \end{aligned} \tag{22}$$

Step 3: The error variables are define as:

$$e_\upsilon = \upsilon - \upsilon_{cf} \quad \zeta_\upsilon = \upsilon_c - \upsilon_{cf} \tag{23}$$

Then a new Lyapunov function can be defined as:

$$V_3 = V_2 + \frac{1}{2}\left(e_\upsilon^2 + \zeta_\upsilon^2\right) \tag{24}$$

Differentiating Eq. (24) along with Eq. (22) yields:

$$\begin{aligned} \dot{V}_3 &= \dot{V}_2 + e_\upsilon\dot{e}_\upsilon + \zeta_\upsilon\dot{\zeta}_\upsilon \\ &= -\lambda_1 e_x^2 - \lambda_2 e_y^2 + e_u(\dot{e}_u - e_x) + \zeta_u\dot{\zeta}_u + \zeta_\upsilon\dot{\zeta}_\upsilon \\ &\quad e_\upsilon(v_m\cos\psi_e(\dot{\psi}_d - r) + \dot{v}_m\sin\psi_e + e_y - \dot{\upsilon}_c) \end{aligned} \tag{25}$$

To ensure $\dot{V}_3 \le 0$, the following desired signals are selected:

$$r_c = \dot{\psi}_d + \frac{\dot{v}_m}{v_m} + \frac{\lambda_3 e_\upsilon + e_y - \dot{\upsilon}_c}{v_m\cos\psi_e} \tag{26}$$

where λ_4 is a positive constant.

Substituting Eq. (26) into Eq. (25) yields:

$$\dot{V}_3 = -\lambda_1 e_x^2 - \lambda_2 e_y^2 - \lambda_3 e_\upsilon^2 + \zeta_u\dot{\zeta}_u + \zeta_\upsilon\dot{\zeta}_\upsilon \tag{27}$$

Step 4: The error variables are defined as:

$$e_r = r - r_{cf} \quad \zeta_r = r_c - r_{cf} \tag{28}$$

Then, a new Lyapunov function can be defined as:

$$V_4 = V_3 + \frac{1}{2}\left(e_r^2 + \zeta_r^2\right) \tag{29}$$

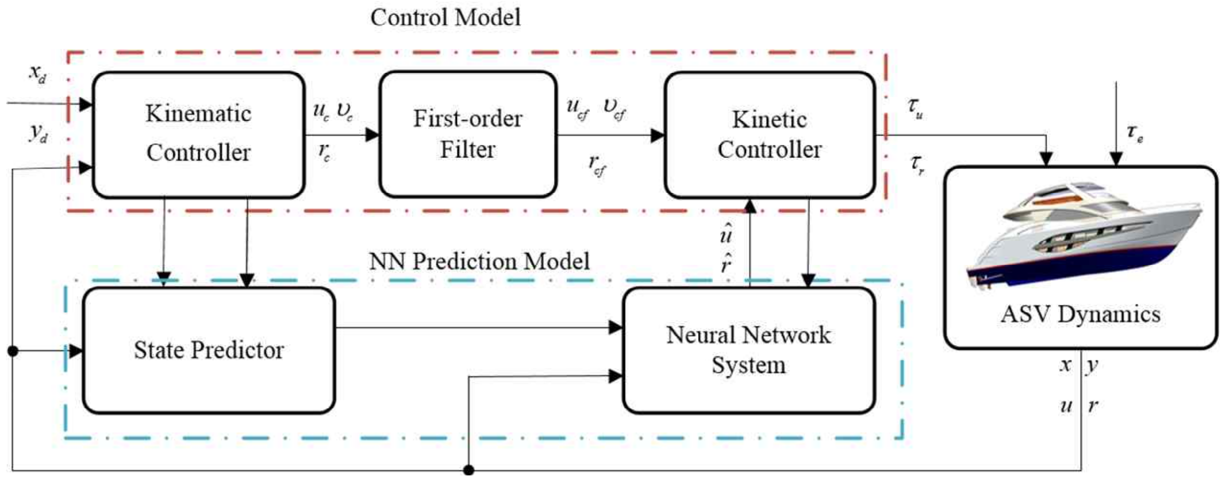

Fig. 3. The block diagram of the proposed method.

Differentiating Eq. (29) along with Eq. (27) yields:

$$\begin{aligned}\dot{V}_4 &= \dot{V}_3 + e_r\dot{e}_r + \zeta_r\dot{\zeta}_r \\ &= -\lambda_1 e_x^2 - \lambda_2 e_y^2 - \lambda_3 e_\upsilon^2 + \zeta_u\dot{\zeta}_u + \zeta_\upsilon\dot{\zeta}_\upsilon + \zeta_r\dot{\zeta}_r \\ &\quad + e_u(\dot{e}_u - e_x) + e_r(\dot{e}_r - e_\upsilon v_m \cos\psi_e)\end{aligned} \tag{30}$$

Step 5: The RBF neural network is used to approximate the unknown function. The unknown functions of underactuated ASVs are expressed as follows:

$$\begin{aligned}\kappa_1 &= m_{22}vr - X_u u - X_{u|u|}u|u| + m_{11}\dot{u}_{cf} \\ \kappa_3 &= (m_{11} - m_{22})uv - N_r r - N_{r|r|}r|r| + m_{33}\dot{r}_{cf}\end{aligned} \tag{31}$$

The prediction error between the system state and the serial-parallel estimation model [34] is considered to improve the tracking performance of the underactuated ASV. The state prediction errors are defined as:

$$\dot{z}_1 = \kappa_1 - \hat{\kappa}_1 \quad \dot{z}_3 = \kappa_3 - \hat{\kappa}_3 \tag{32}$$

The control inputs are designed as:

$$\begin{aligned}\tau_u &= -m_{11}(\alpha_1 e_u + e_x) + \\ &\qquad \hat{\mathbf{W}}_1\mathbf{h}(\mathbf{x}_u) + \mu_1 z_1 - \hat{\sigma}_u \tanh(v\hat{\sigma}_u e_u / \gamma_u) \\ \tau_r &= -m_{33}(\alpha_3 e_r + e_\upsilon v_m \cos\psi_e) + \\ &\qquad \hat{\mathbf{W}}_3\mathbf{h}(\mathbf{x}_r) + \mu_3 z_3 - \hat{\sigma}_r \tanh(v\hat{\sigma}_r e_r / \gamma_r)\end{aligned} \tag{33}$$

where α_1, μ_1, γ_u, α_3, μ_3, γ_r are positive constants.

The prediction errors are used to construct the learning design, so the NN updating law are selected as:

$$\begin{aligned}\dot{\hat{\mathbf{W}}}_1 &= \beta_1\left[(e_u + \delta_1 z_1)\mathbf{h}(\mathbf{x}_u) - \chi_1\hat{\mathbf{W}}_1\right] \\ \dot{\hat{\mathbf{W}}}_3 &= \beta_3\left[(e_r + \delta_3 z_3)\mathbf{h}(\mathbf{x}_r) - \chi_3\hat{\mathbf{W}}_3\right]\end{aligned} \tag{34}$$

where β_1, δ_1, χ_1, β_3, δ_3, χ_3 are positive constants.

The sliding mode control is combined with adaptive techniques to compensate the nonlinear external disturbances. The adaptive laws are selected as:

$$\begin{aligned}\dot{\hat{\sigma}}_u &= \rho_1|e_u| - \rho_1\vartheta_1(\hat{\sigma}_u - \sigma_{u0}) \\ \dot{\hat{\sigma}}_r &= \rho_3|e_r| - \rho_3\vartheta_3(\hat{\sigma}_r - \sigma_{r0})\end{aligned} \tag{35}$$

where ρ_1, ϑ_1, σ_{u0}, ρ_3, ϑ_3, σ_{r0} are positive constants.

Substituting Eq. (33) into Eq. (4) yields:

$$\begin{aligned}m_{11}\dot{e}_u &= -m_{11}(\alpha_1 e_u + e_x) + \hat{\mathbf{W}}_1\mathbf{h}(\mathbf{x}_u) + \mu_1 z_1 - \kappa_1 + \\ &\qquad \tau_{eu} - \hat{\sigma}_u \tanh(v\hat{\sigma}_u e_u / \gamma_u) \\ m_{33}\dot{e}_r &= -m_{33}(\alpha_3 e_r + e_\upsilon v_m \cos\psi_e) + \hat{\mathbf{W}}_3\mathbf{h}(\mathbf{x}_r) + \mu_3 z_3 \\ &\qquad - \kappa_3 + \tau_{er} - \hat{\sigma}_r \tanh(v\hat{\sigma}_r e_r / \gamma_r)\end{aligned} \tag{36}$$

where γ_u, γ_r are positive constants.

Substituting Eq. (36) into Eq. (30) yields:

$$\begin{aligned}\dot{V}_4 &= -\lambda_1 e_x^2 - \lambda_2 e_y^2 - \lambda_3 e_\upsilon^2 - \alpha_1 e_u^2 - \alpha_3 e_r^2 + \zeta_u\dot{\zeta}_u + \zeta_\upsilon\dot{\zeta}_\upsilon + \zeta_r\dot{\zeta}_r \\ &\quad - e_u\tilde{\mathbf{W}}_1\mathbf{h}(\mathbf{x}_u) - e_u\hat{\sigma}_u \tanh(v\hat{\sigma}_u e_u / \gamma_u) - e_u(\tau_{eu} + \varepsilon_u) \\ &\quad - e_r\tilde{\mathbf{W}}_3\mathbf{h}(\mathbf{x}_r) - e_r\hat{\sigma}_r \tanh(v\hat{\sigma}_r e_r / \gamma_r) - e_r(\tau_{er} + \varepsilon_r)\end{aligned} \tag{37}$$

Fig. 3 provides the block diagram of the designed position tracking control scheme for an underactuated ASV.

4. Stability analysis of the overall control system

In this section, the Lyapunov stability theory is employed to prove the stability of the closed-loop control system.

A new Lyapunov function is defined as the following:

$$V_5 = V_4 + \frac{1}{2m_{11}\beta_1}\tilde{\mathbf{W}}_1^T\tilde{\mathbf{W}}_1 + \frac{1}{2m_{33}\beta_3}\tilde{\mathbf{W}}_3^T\tilde{\mathbf{W}}_3 + \frac{1}{2}\delta_1 z_1^2 + \frac{1}{2}\delta_3 z_3^2$$
$$\frac{1}{2m_{11}\rho_1}\tilde{\sigma}_u^2 + \frac{1}{2m_{33}\rho_3}\tilde{\sigma}_r^2 \quad (38)$$

Differentiating Eq. (38) yields:

$$\dot{V}_5 = \dot{V}_4 - \frac{\tilde{\mathbf{W}}_1^T\dot{\hat{\mathbf{W}}}_1}{\beta_1} - \frac{\tilde{\mathbf{W}}_3^T\dot{\hat{\mathbf{W}}}_3}{\beta_3} - \delta_1 z_1\dot{z}_1 - \delta_3 z_3\dot{z}_3 - \frac{\tilde{\sigma}_u\dot{\hat{\sigma}}_u}{\rho_1} - \frac{\tilde{\sigma}_r\dot{\hat{\sigma}}_r}{\rho_3} \quad (39)$$

The state prediction errors can be expressed as:

$$\begin{aligned}\dot{z}_1 &= \kappa_1 - \hat{\kappa}_1 = \tilde{\mathbf{W}}_1\mathbf{h}(\mathbf{x}_u) + \varepsilon_u - \delta_1 z_1\\ \dot{z}_3 &= \kappa_3 - \hat{\kappa}_3 = \tilde{\mathbf{W}}_3\mathbf{h}(\mathbf{x}_r) + \varepsilon_r - \delta_3 z_3\end{aligned} \quad (40)$$

Then, the correlations can be obtained as:

$$\begin{aligned}z_1\dot{z}_1 &= z_1\tilde{\mathbf{W}}_1\mathbf{h}(\mathbf{x}_u) + z_1\varepsilon_u - \delta_1 z_1^2\\ z_3\dot{z}_3 &= z_3\tilde{\mathbf{W}}_3\mathbf{h}(\mathbf{x}_r) + z_3\varepsilon_r - \delta_3 z_3^2\end{aligned} \quad (41)$$

Substituting Eqs. (34), (37) and (41) into Eq. (39) yields:

$$\begin{aligned}\dot{V}_5 = &-\lambda_1 e_x^2 - \lambda_2 e_y^2 - \lambda_3 e_u^2 - \lambda_4 e_\upsilon^2 + \zeta_u\dot{\zeta}_u + \zeta_\upsilon\dot{\zeta}_\upsilon + \zeta_r\dot{\zeta}_r\\ &-(e_u + \delta_1 z_1)\tilde{\mathbf{W}}_1\mathbf{h}(\mathbf{x}_u) + \chi_1\tilde{\mathbf{W}}_1^T\hat{\mathbf{W}}_1\\ &-e_u\hat{\sigma}_u\tanh(v\hat{\sigma}_u e_u/\gamma_u) - e_u(\tau_{eu} + \varepsilon_u)\\ &-(e_r + \delta_3 z_3)\tilde{\mathbf{W}}_3\mathbf{h}(\mathbf{x}_r) + \chi_3\tilde{\mathbf{W}}_3^T\hat{\mathbf{W}}_3\\ &-e_r\hat{\sigma}_r\tanh(v\hat{\sigma}_r e_r/\gamma_r) - e_r(\tau_{er} + \varepsilon_r)\\ &+\delta_1 z_1\tilde{\mathbf{W}}_1\mathbf{h}(\mathbf{x}_u) + \delta_1 z_1\varepsilon_1 - \delta_1 z_1^2\\ &+\delta_3 z_3\tilde{\mathbf{W}}_3\mathbf{h}(\mathbf{x}_r) + \delta_3 z_3\varepsilon_3 - \delta_3 z_3^2\\ &-\frac{\tilde{\sigma}_u\hat{\sigma}_u}{\rho_1} - \frac{\tilde{\sigma}_r\hat{\sigma}_r}{\rho_3}\end{aligned} \quad (42)$$

Moreover, substituting Eq. (35) into Eq. (42) yields:

$$\begin{aligned}\dot{V}_5 = &-\lambda_1 e_x^2 - \lambda_2 e_y^2 - \lambda_3 e_u^2 - \lambda_4 e_\upsilon^2 + \varepsilon_u\dot{\varepsilon}_u + \varepsilon_\upsilon\dot{\varepsilon}_\upsilon + \varepsilon_r\dot{\varepsilon}_r\\ &-e_u\hat{\sigma}_u\tanh(v\hat{\sigma}_u e_u/\gamma_u) - e_u(\tau_{eu} + \varepsilon_u)\\ &-e_r\hat{\sigma}_r\tanh(v\hat{\sigma}_r e_r/\gamma_r) - e_r(\tau_{er} + \varepsilon_r)\\ &e_u\tilde{\mathbf{W}}_1\mathbf{h}(\mathbf{x}_u) + \chi_1\tilde{\mathbf{W}}_1^T\hat{\mathbf{W}}_1 + e_r\tilde{\mathbf{W}}_3\mathbf{h}(\mathbf{x}_r) + \chi_3\tilde{\mathbf{W}}_3^T\hat{\mathbf{W}}_3\\ &+\delta_1 z_1\varepsilon_1 - \delta_1 z_1^2 + \delta_3 z_3\varepsilon_3 - \delta_3 z_3^2\\ &-\tilde{\sigma}_1|e_u| + \tilde{\sigma}_u(\hat{\sigma}_u - \sigma_{u0}) - \tilde{\sigma}_r|e_r| + \tilde{\sigma}_r(\hat{\sigma}_r - \sigma_{r0})\end{aligned} \quad (43)$$

Based on Eq. (43), the following correlations can be obtained:

$$\begin{aligned}z_1\varepsilon_u - \mu_1 z_1^2 &= -\mu_1\left(z_1 - \frac{\varepsilon_u}{2\mu_1}\right)^2 + \frac{1}{4\mu_1}\varepsilon_u^2\\ z_3\varepsilon_r - \mu_3 z_r^2 &= -\mu_3\left(z_3 - \frac{\varepsilon_r}{2\mu_3}\right)^2 + \frac{1}{4\mu_3}\varepsilon_r^2\end{aligned} \quad (44)$$

Then, the following equations are obtained:

$$\begin{aligned}\tilde{\mathbf{W}}_1^T\mathbf{W}_1^* - \tilde{\mathbf{W}}_1^T\mathbf{W}_1 &= -\left\|\tilde{\mathbf{W}}_1 - \frac{\mathbf{W}_1^*}{2}\right\|^2 + \frac{1}{4}\left\|\mathbf{W}_1^*\right\|^2\\ \tilde{\mathbf{W}}_3^T\mathbf{W}_3^* - \tilde{\mathbf{W}}_3^T\mathbf{W}_3 &= -\left\|\tilde{\mathbf{W}}_3 - \frac{\mathbf{W}_3^*}{2}\right\|^2 + \frac{1}{4}\left\|\mathbf{W}_3^*\right\|^2\end{aligned} \quad (45)$$

Substituting Eqs. (44) and (45) into Eq. (43) yields:

$$\begin{aligned}\dot{V}_5 = &-\lambda_1 e_x^2 - \lambda_2 e_y^2 - \lambda_3 e_u^2 - \lambda_4 e_\upsilon^2 + \zeta_u\dot{\zeta}_u + \zeta_\upsilon\dot{\zeta}_\upsilon + \zeta_r\dot{\zeta}_r\\ &-e_u\hat{\sigma}_u\tanh(v\hat{\sigma}_u e_u/\gamma_u) - e_u(\tau_{eu} + \varepsilon_u)\\ &-e_r\hat{\sigma}_r\tanh(v\hat{\sigma}_r e_r/\gamma_r) - e_r(\tau_{er} + \varepsilon_r)\\ &-\tilde{\sigma}_u|e_u| + \tilde{\sigma}_u(\hat{\sigma}_u - \sigma_{u0}) - \tilde{\sigma}_r|e_r| + \tilde{\sigma}_r(\hat{\sigma}_r - \sigma_{r0})\\ &-\chi_1\left[\left\|\tilde{\mathbf{W}}_1 - \frac{\mathbf{W}_1^*}{2}\right\|^2 - \frac{1}{4}\left\|\mathbf{W}_1^*\right\|^2\right]\\ &-\chi_3\left[\left\|\tilde{\mathbf{W}}_3 - \frac{\mathbf{W}_3^*}{2}\right\|^2 - \frac{1}{4}\left\|\mathbf{W}_3^*\right\|^2\right]\\ &-\delta_1\left[\mu_1\left(z_1 - \frac{\varepsilon_u}{2\mu_1}\right)^2 - \frac{1}{4\mu_1}\varepsilon_u^2\right]\\ &-\delta_3\left[\mu_3\left(z_3 - \frac{\varepsilon_r}{2\mu_3}\right)^2 - \frac{1}{4\mu_3}\varepsilon_r^2\right]\end{aligned} \quad (46)$$

Lemma 1. The relation $h|x| \le xh\tanh(vhx/\mu_t)$ ensures that for any $\mu_t > 0$ and for any $\forall x \in R, h \in R$, v satisfies $v = e^{-(v+1)}$, $i.e.\ v = 0.2785$ [20].

According to lemma 1, the following inequality can be obtained:

$$\begin{aligned}\hat{\sigma}_u|e_u| &\le e_u\hat{\sigma}_u\tanh(v\hat{\sigma}_u e_u/\gamma_u) + \mu_u\\ \hat{\sigma}_r|e_r| &\le e_r\hat{\sigma}_r\tanh(v\hat{\sigma}_r e_r/\gamma_r) + \mu_r\end{aligned} \quad (47)$$

According to assumptions 1 and 2, the external disturbances and the approximation errors are bounded. It is assumed that:

$$\begin{aligned}|\tau_{eu} + \varepsilon_u| &\le \sigma_u\\ |\tau_{er} + \varepsilon_r| &\le \sigma_r\end{aligned} \quad (48)$$

According to Shojaei's study [35], it is obtained as:

$$\begin{aligned}\tilde{\sigma}_u(\hat{\sigma}_u - \sigma_{u0}) &\le -q_1|\tilde{\sigma}_u^2| + q_2|\sigma_u - \sigma_{u0}|^2\\ \tilde{\sigma}_r(\hat{\sigma}_r - \sigma_{r0}) &\le -q_1|\tilde{\sigma}_r^2| + q_2|\sigma_r - \sigma_{r0}|^2\end{aligned} \quad (49)$$

where $q_1 = 1 - 0.5/\ell^2$, $q_2 = 0.5/\ell^2$ and $\ell > \sqrt{2}/2$.

Substituting Eqs. (47), (48) and (49) into Eq. (47) yields:

$$
\begin{aligned}
\dot{V}_5 \le & -\lambda_1 e_x^2 - \lambda_2 e_y^2 - \lambda_3 e_u^2 - \lambda_4 e_\upsilon^2 + \zeta_u \dot{\zeta}_u + \zeta_\upsilon \dot{\zeta}_\upsilon + \zeta_r \dot{\zeta}_r \\
& - \delta_{\min}\mu_{\min}\left[\left(z_1 - \frac{\varepsilon_u}{2\mu_1}\right)^2 + \left(z_3 - \frac{\varepsilon_r}{2\mu_3}\right)^2\right] \\
& - \chi_{\min}\left[\left\|\tilde{\mathbf{W}}_1 - \frac{\mathbf{W}_1^*}{2}\right\|^2 + \left\|\tilde{\mathbf{W}}_3 - \frac{\mathbf{W}_3^*}{2}\right\|^2\right] \\
& - q_1\mathbb{J}_1\left|\tilde{\sigma}_u^2\right| - q_3\mathbb{J}_3\left|\tilde{\sigma}_r^2\right| \\
& + \frac{\delta_{\max}}{2\mu_{\min}}\varepsilon_M^2 + \frac{\chi_{\max}}{2}W_M^2 \\
& + q_1\mathbb{J}_1\left|\sigma_u - \sigma_{u0}\right|^2 + q_3\mathbb{J}_3\left|\sigma_r - \sigma_{r0}\right|^2
\end{aligned} \tag{50}
$$

Differentiating Eqs. (19),(20) and (25) yields:

$$
\begin{aligned}
\dot{\zeta}_u &= \dot{u}_{cf} - \dot{u}_c = -\zeta_u / k_u + du_c / dt \\
\dot{\zeta}_\upsilon &= \dot{\upsilon}_{cf} - \dot{\upsilon}_c = -\zeta_\upsilon / k_\upsilon + d\upsilon_c / dt \\
\dot{\zeta}_r &= \dot{r}_{cf} - \dot{r}_c = -\zeta_r / k_r + dr_c / dt
\end{aligned} \tag{51}
$$

According to Shojaei's study [35], it is obtained as

$$
\left|du_c / dt\right| \le \varpi_u, \left|d\upsilon_c / dt\right| \le \varpi_\upsilon, \left|dr_c / dt\right| \le \varpi_r \tag{52}
$$

where ϖ_u , ϖ_υ , ϖ_r are positive constants.

Substituting Eq. (52) into Eq. (51) yields:

$$
\begin{aligned}
\zeta_u \dot{\zeta}_u &\le -\zeta_u^2 / k_u + \varpi_u \left|\varpi_u\right| \le -\zeta_u^2 / k_u + \zeta_u^2 + 0.25\varpi_u^2 \\
\zeta_\upsilon \dot{\zeta}_\upsilon &\le -\zeta_\upsilon^2 / k_\upsilon + \varpi_\upsilon \left|\varpi_\upsilon\right| \le -\zeta_\upsilon^2 / k_\upsilon + \zeta_\upsilon^2 + 0.25\varpi_\upsilon^2 \\
\zeta_r \dot{\zeta}_r &\le -\zeta_r^2 / k_r + \varpi_r \left|\varpi_r\right| \le -\zeta_r^2 / k_r + \zeta_r^2 + 0.25\varpi_r^2
\end{aligned} \tag{53}
$$

Moreover, substituting Eq. (53) into Eq. (50) yields:

$$
\begin{aligned}
\dot{V}_5 \le & -\lambda_1 e_x^2 - \lambda_2 e_y^2 - \lambda_3 e_u^2 - \lambda_4 e_\upsilon^2 - q_1\mathbb{J}_1\left|\tilde{\sigma}_u^2\right| - q_3\mathbb{J}_3\left|\tilde{\sigma}_r^2\right| \\
& -\left(1 - \frac{1}{k_u}\right)\zeta_u^2 - \left(1 - \frac{1}{k_\upsilon}\right)\zeta_\upsilon^2 - \left(1 - \frac{1}{k_r}\right)\zeta_r^2 \\
& - \delta_{\min}\mu_{\min}\left[\left(z_1 - \frac{\varepsilon_u}{2\mu_1}\right)^2 + \left(z_3 - \frac{\varepsilon_r}{2\mu_3}\right)^2\right] \\
& - \chi_{\min}\left[\left\|\tilde{\mathbf{W}}_1 - \frac{\mathbf{W}_1^*}{2}\right\|^2 + \left\|\tilde{\mathbf{W}}_3 - \frac{\mathbf{W}_3^*}{2}\right\|^2\right] \\
& + \frac{\delta_{\max}}{2\mu_{\min}}\varepsilon_M^2 + \frac{\chi_{\max}}{2}W_M^2 + 0.25\left({}_u^2 + {}_\upsilon^2 + {}_r^2\right) \\
& + q_1\mathbb{J}_1\left|\sigma_u - \sigma_{u0}\right|^2 + q_3\mathbb{J}_3\left|\sigma_r - \sigma_{r0}\right|^2
\end{aligned} \tag{54}
$$

Then, the $\dot{V}_5$ can be expressed as the following:

$$
\dot{V}_5 \le -2\xi V_5 + \Phi \tag{55}
$$

where

$$
\begin{aligned}
\xi = \min\{ & \lambda_1, \lambda_2, \lambda_3, \lambda_4, q_1\vartheta_1, q_3\vartheta_3, \\
& 1 - \frac{1}{k_u}, 1 - \frac{1}{k_\upsilon}, 1 - \frac{1}{k_r}, \delta_{\min}\mu_{\min}, \chi_{\min}\} \\
\Phi = & \frac{\delta_{\max}}{2\mu_{\min}}\varepsilon_M^2 + \frac{\chi_{\max}}{2}W_M^2 + 0.25\left(\varpi_u^2 + \varpi_\upsilon^2 + \varpi_r^2\right) \\
& + q_1\vartheta_1\left|\sigma_u - \sigma_{u0}\right|^2 + q_3\vartheta_3\left|\sigma_r - \sigma_{r0}\right|^2 + \mu_u + \mu_r
\end{aligned}
$$

Eq. (55) can be converted to the following equation:

$$
V \le \frac{\Phi}{2\xi} + \left[V(0) - \frac{\Phi}{2\xi}\right]e^{-2\xi t} \tag{56}
$$

The equality can be obtained as:

$$
\lim_{t\to\infty} V = \frac{\Phi}{2\xi} \tag{57}
$$

In summary, all error signals for the overall closed-loop control system are uniformly bounded in the abovemetioned results. The position tracking errors converge to a small neighborhood of the zero.

5. Simulation and comparative analysis

In this section, the efficiency of the proposed robust controller is discussed by comparing it with the conventional backstepping method using the MATLAB software environment. In order to prove the performance of the designed controller, the simulations are performed on an underactuated ASV designed by the University of Western Australia. It is assumed that the mass and the damping matrices are diagonal. Model parameters are shown in Ref. [36].

Assume that the tracking trajectory of the underactuated ASV is as follows:

$$
\begin{aligned}
x_d &= 10\sin(0.01t)m / s \\
y_d &= 10\cos(0.01t)m / s
\end{aligned} \tag{58}
$$

In order to realize the position tracking and gurantee the application in practice, the initial conditions of the underactuated ASV are selected as the following:

$$
\begin{aligned}
& x(0) = -5m \text{ , } y(0) = 5m \text{ , } \psi(0) = 0rad \\
& u(0) = 0.4m / s \text{ , } v(0) = 0m / s \text{ , } r(0) = 0rad / s
\end{aligned}
$$

In practical underactuated ASVs system, the control inputs are constrained so that the control input system can be protected. For the selected underactuated ASVs system, the input constraint are described as the following:

$$
0 \le \left|\tau_u\right| \le 30N \text{ , } 0 \le \left|\tau_r\right| \le 20N \cdot m
$$

In order to represent the tracking error clearly, a new trajec-

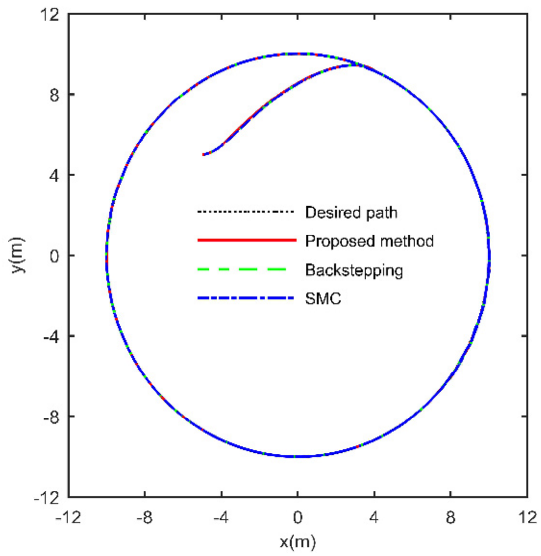

Fig. 4. Position tracking of the underactuated ASV.

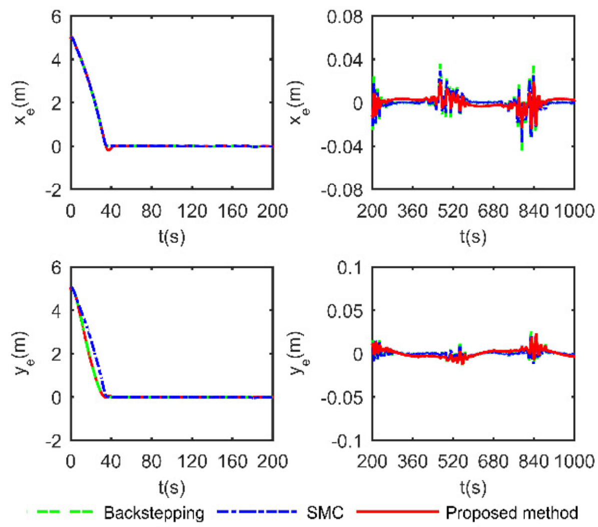

Fig. 5. The errors of the position tracking of the underactuated ASV.

tory tracking error variable is defined as:

$$L = \sqrt{x_e^2 + y_e^2} \tag{59}$$

To verify the control performance and effectiveness of the designed control system, the nonlinear external disturbances are selected as:

$$\boldsymbol{d}(t) + \boldsymbol{P}\dot{\boldsymbol{d}}(t) = \boldsymbol{T}\omega \tag{60}$$

where $\boldsymbol{d}(t) = [\tau_{eu}, \tau_{ev}, \tau_{er}]^T$. Moreover, $\boldsymbol{P}$, ω and $\boldsymbol{T}$ denote the time constant matrix, the white high frequency measurement noise and the gain parameters matrix, respectively. Considering the worst case, $\boldsymbol{P} = \text{diag}\{100, 100, 100\}$, $\omega = 1$ and $\boldsymbol{T} = \text{diag}\{10, 5, 10\}$ are selected.

In this numerical simulation, the control parameters are given by $\lambda_1 = 0.5$, $\lambda_2 = 0.4$, $\lambda_3 = 0.3$, $\lambda_4 = 0.2$, $\alpha_5 = 1$, $\gamma_u = 0.1$, $\gamma_\kappa = 0.1$, $\gamma_r = 0.1$, $\eta_1 = 0.2$, $\eta_3 = 0.2$, $\rho_1 = 0.3$, $\rho_3 = 0.2$, $\mathbb{J}_1 = 0.2$, $\vartheta_3 = 0.2$.

Moreover, the parameters of the RBF neural network with five hidden nodes designed in the present study are given by $\beta_1 = 30$, $\beta_3 = 30$, $\chi_1 = 0.1$, $\chi_3 = 0.1$, $\delta_1 = 0.2$, $\delta_3 = 0.2$. The standard deviation and the centre vector are selected as $\boldsymbol{b}_j = 15$ and $\boldsymbol{c}_j = [-1.0\ \ -0.5\ \ 0\ \ 0.5\ \ 1.0]$, respectively.

Finally, to express the control performance, the simulation time is set to 1000 s. Figs. 5-8 show the simulation results of the proposed method, the conventional backstepping method, and sliding mode control [37].

Figs. 4 and 5 illustrate that the proposed method has better tracking performance than the backstepping method and the sliding mode control method in the presence of the parameters uncertainties and nonlinear external disturbances for the un-

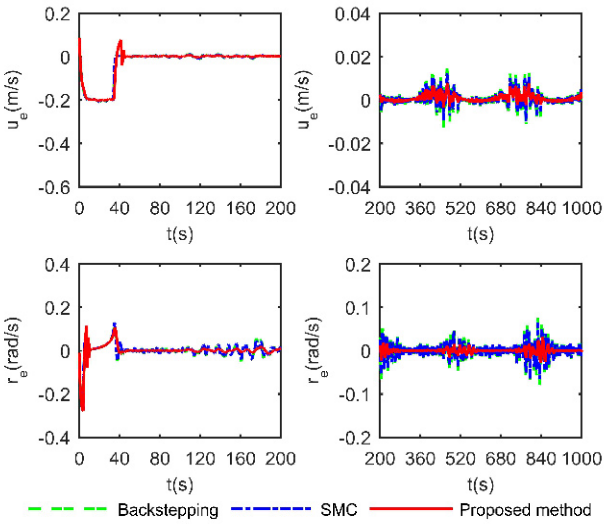

Fig. 6. The errors of the velocity tracking of the underactuated ASV.

deractuated ASV. Moreover, the absolute value of tracking errors can be obtained every 40 s from 200 s to 1000 s. The average tracking error of the backstepping mehod, sliding mode control and the proposed method are 0.0060 m, 0.0055 m and 0.0042 m, respectively. Furthermore, Fig. 6 shows that the velocity can track the desired variables rapidly. It should be indicated that the velocity tracking errors of proposed method are significantly smaller than those of the backstepping method and sliding mode control.

Fig. 7 shows the control inputs of the underactuated ASV. The absolute value of control inputs can be obtained every 40 s from 200 s to 1000 s. The average control forces of the backstepping method, sliding mode control and the proposed method are 9.2 N, 8.5 N, and 8.1 N, respectively. Moreover, it is observed that the average control moments of the backstepping method, sliding mode control and proposed method are

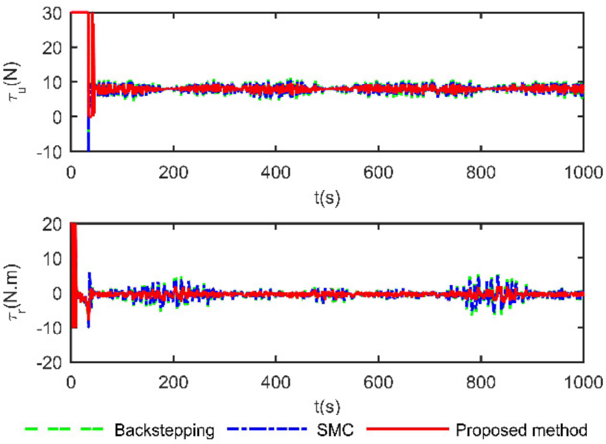

Fig. 7. The control force and moment of the underactuated ASV.

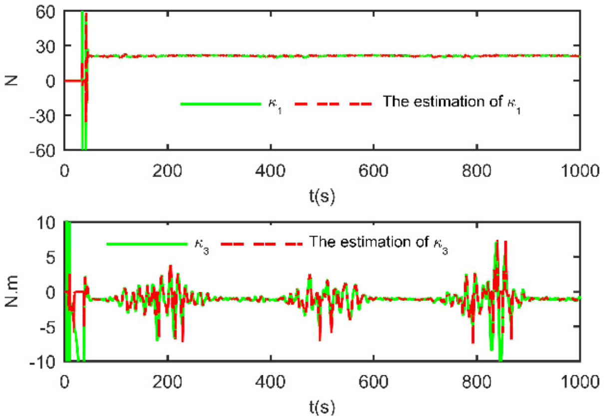

Fig. 8. The estimated uncertainties with the RBF neural network.

6.3 N.m, 5.0 N.m and 4.5 N.m, respectively. It should be indicated that the chattering is obviously reduced in the control force and control moment.

All unknown model parameters can be approximated accurately by employing the RBF neural network and state predictors in Fig. 8.

6. Conclusion

In the present study, the position tracking control problem of the underactuated ASV is investigated in the presence of the model parameters uncertainties and the nonlinear external disturbances. Moreover, an adaptive neural network robust control scheme is proposed to deal with the multiple uncertainties and the nonlinear external disturbances. The derivative of virtual control variables are obtained by applying the dynamic surface control, which avoids the computational complexities of the conventional backstepping method. Furthermore, the stability of the closed-loop control system is proved by the Lyapunov stability theory. Finally, the reasonable robustness and effectiveness of the designed controller are shown in the simulation results.

Acknowledgments

The authors acknowledge support by the National Natural Science Foundation of China (NSFC, Grant Nos. 11672094).

References

[1] E. Fredriksen and K. Y. Petterson, Global k-exponential way-point maneuvering of ships: Theory and experiments, *Automatica*, 42 (4) (2006) 677-687.

[2] M. Chen, S. S. Ge, B. V. E. How and Y. S. Choo, Robust adaptive position mooring control for marine vessels, *IEEE Transactions on Control Systems Technology*, 21 (2) (2013) 395-409.

[3] J. Gao, A. A. Proctor, Y. Shi and C. Bradley, Hierarchical model predictive image-based visual servoing of underwater vehicles with adaptive neural network dynamic control, *IEEE Transactions on Cybernetics*, 46 (10) (2016) 2323-2334.

[4] S. R. Oh and J. Sun, Path following of underactuated marine surface vessels using line-of-sight based model predictive control, *Ocean Engineering*, 37 (2) (2010) 289-295.

[5] K. Shojaei, Observer-based neural adaptive formation control of autonomous surface vessels with limited torque, *Robotics and Autonomous Systems*, 78 (2) (2016) 83-96.

[6] Z. Zhao, W. He and S. S. Ge, Adaptive neural network control of a fully actuated marine surface vessel with multiple output constraints, *IEEE Transactions on Control Systems Technology*, 22 (4) (2014) 1536-1543.

[7] M. Wondergem, E. Lefeber, K. Y. Pettersen and H. Nijmeijer, Output feedback tracking of ships, *IEEE Transactions on Control Systems Technology*, 19 (2) (2011) 442-448.

[8] A. Thakur, P. Svec and S. K. Gupta, GPU based generation of state transition models using simulations for unmanned surface vehicle trajectory planning, *Robotics and Autonomous Systems*, 60 (12) (2012) 1457-1471.

[9] M. E. Serrano, G. J. E. Scaglia, S. A. Godoy, V. Mut and O. Ortiz, Trajectory tracking of underactuated surface vessels: A linear algebra approach, *IEEE Transactions on Control Systems Technology*, 22 (3) (2014) 1103-1111.

[10] L. Liu, D. Wang and Z. H. Peng, Path following of marine surface vehicles with dynamical uncertainty and time-varying ocean disturbances, *Neurocomputing*, 173 (2016) 799-808.

[11] L. Liu, D. Wang, Z. H. Peng and H. Wang, Predictor-based LOS guidance law for path following of underactuated marine surface vehicles with sideslip compensation, *Ocean Engineering*, 124 (2016) 340-348.

[12] F. Y. Bi , Y. J. Wei, J. Z. Zhang and W. Cao, Position tracking control of underactuated autonomous underwater vehicles in the presence of unknown ocean currents, *IET Control Theory and Applications*, 4 (11) (2010) 2369-2380.

[13] C. Z. Pan, X. Z. Lai, S. X. Yang and M. Wu, A biologically inspired approach to tracking control of underactuated surface vessels subject to unknown dynamics, *Expert Systems with Applications*, 42 (4) (2015) 2153-2161.

[14] C. Z. Pan, S. X. Yang, X. Z. Lai and L. Zhou, An efficient neural network based tracking controller for autonomous underwater vehicles subject to unknown dynamics, *Control and Decision Conference*, *IEEE* (2014) 3300-3305.

[15] C. Z. Pan, X. Z. Lai, S. X. Yang and M. Wu, A bioinspired neural dynamics-based approach to tracking control of autonomous surface vehicles subject to unknown ocean currents, *Neural Computing and Applications*, 26 (8) (2015) 1929-1938.

[16] K. D. Do, Z. P. Jiang and J. Pan, Robust adaptive path following of underactuated ships, *Automatica*, 40 (6) (2004) 929-944.

[17] K. D. Do and J. Pan, Global tracking control of underactuated ships with nonzero off-diagonal terms in their system matrices, *Automatica*, 41 (1) (2005) 87-95.

[18] W. J. Xie , B. L. Ma, W. Huang and Y. X. Zhao, Global trajectory tracking control of underactuated surface vessels with non-diagonal inertial and damping matrices, *Nonlinear Dynamics*, 92 (2018) 1481-1492.

[19] D. Swaroop et al., Dynamic surface control for a class of nonlinear systems, *IEEE Transactions on Automatic Control*, 45 (10) (2000) 1893-1899.

[20] J. Q. Wang, C. Wang, Y. J. Wei and C. J. Zhang, Command filter based adaptive neural trajectory tracking control of an underactuated underwater vehicle in three-dimensional space, *Ocean Engineering*, 180 (2019) 175-186.

[21] J. Q. Wang, C. Wang, Y. J. Wei and C. J. Zhang, Three-dimensional path following of an underactuated AUV based on neuro-adaptive command filtered backstepping control, *IEEE Access*, 6 (2018) 74355-74365.

[22] J. Q. Wang, C. Wang, Y. J. Wei and C. J. Zhang, Position tracking control of autonomous underwater vehicles in the disturbance of unknown ocean currents, *ACTA ARMAMENTARII*, 3 (40) (2019) 583-591.

[23] Z. Zheng and L. Sun, Path following control for marine surface vessel with uncertainties and input saturation, *Neurocomputing*, 177 (2016) 158-167.

[24] N. Wang and J. E. Meng, Direct adaptive fuzzy tracking control of marine vehicles with fully unknown parametric dynamics and uncertainties, *IEEE Transactions on Control Systems Technology*, 24 (5) (2016) 1845-1852.

[25] X. Liang, X. J. Hua, L. F. Su, W. Li and J. D. Zhang, Path following control for underactuated AUV based on feedback gain backstepping, *Technical Gazette*, 22 (4) (2015) 829-835.

[26] H. J. Wang, Z. Y. Chen, H. M. Jia, J. Li and X. H. Chen, Three-dimensional path following control of underactuated autonomous underwater vehicle with command filtered backstepping, *Acta Automatica Sinica*, 41 (3) (2015) 631-645.

[27] H. Wang, D. Wang and Z. H. Peng, Neural network based adaptive dynamic surface control for cooperative path following of marine surface vehicles via state and output feedback, *Neurocomputing*, 133 (2014) 170-178.

[28] Z. W. Zheng, Y. T. Huang, L. H. Xie and B. Zhu, Adaptive trajectory tracking control of a fully actuated surface vessel with asymmetrically constrained input and output, *IEEE Transactions on Control System Technology*, 26 (5) (2018) 1851-1859.

[29] B. S. Park, J. W. Kwon and H. Kim, Neural network-based output feedback control for reference tracking of underactuated surface vessels, *Automatica*, 77 (2017) 353-359.

[30] L. Liu, D. Wang and Z. Peng, Coordinated path following of multiple underacutated marine surface vehicles along one-curve, *ISA Transactions*, 64 (2016) 258-268.

[31] R. Sanner and J. Slotine, Gaussian networks for direct adaptive control, *IEEE Transations on Neural Network*, 3 (1992) 837-863.

[32] K. Shojaei, Leader - follower formation control of underactuated autonomous marine surface vehicles with limited torque, *Ocean Engineering*, 105 (2015) 196-205.

[33] D. Swaroop, J. Hedrick, P. Yip and J. Gerdes, Dynamic surface control for a class of nonlinear systems, *IEEE Transactions Automation Control*, 45 (2000) 1893-1899.

[34] B. Xu, C. G. Yang and F. C. Sun, Composite neural dynamic surface control of a class of uncertain nonlinear systems in strict-feedback form, *IEEE Transactions on Cybernetics*, 44 (2014) 2626-2634.

[35] K. Shojaei, Line-of-sight target tracking control of underactuated autonomous underwater vehicles, *Ocean Engineering*, 133 (2017) 244-252.

[36] M. Reyhanoglu, Exponential stabilization of an underactuated autonomous surface vessel, *Automatica*, 33 (12) (1997) 2249-2254.

[37] F. Y. Bi , Y. J. Wei, J. Z. Zhang and W. Cao, Robust position tracking control design for underactuated AUVs, *Journal of Harbin Insititute of Technology*, 42 (11) (2010) 1690-1695.

Chengju Zhang was born in Puyang, Henan Province, China. He received the B.E. degree in Naval Architecture and Ocean Engineering from the School of Shipbuilding Engineering, Harbin Engineering University, Harbin, China, in 2017. He is now pursuing his Ph.D. degree in Astronautics at Harbin Institute of Technology. His current research interests include the motion control of marine surface vehicles.

Cong Wang received his Ph.D. degree in Mechanics from Harbin Institute of Technology, Harbin, China, in 2001. He received his Bachelor and Master degrees in Mechanical and Electrical Engineering from Northeast Forestry University in 1989 and 1993, respectively. He is currently a Professor at School of Astronautics, Harbin Institute of Technology, China. His current research interests include fluid mechanics and the motion control of underwater vehicles.

Yingjie Wei received his Ph.D. degree in Mechanics from Harbin Institute of Technology, Harbin, China, in 2003. He received his Bachelor and Master degrees in Oil and Gas Field Development from the Northeast Petroleum University in 1996 and 2000, respectively. He is currently a Professor at School of Astronautics, Harbin Institute of Technology, China. His current research interests include multiphase fluid mechanics and hydrodynamics of the underwater vehicles.

Jinqiang Wang was born Harbin, Heilongjiang Province, China. He received the B.E. degree in Naval Architecture and Ocean Engineering from the School of Shipbuilding Engineering, Harbin Engineering University, Harbin, China, in 2016. He is now pursuing his Ph.D. degree in Astronautics at Harbin Institute of Technology. His current research interests include guidance and the motion control of autonomous underwater vehicles.